Available online at www.sciencedirect.com
ScienceDirect
Ceramics International 33 (2007) 1403–1407
CERAMICS INTERNATIONAL
www.elsevier.com/locate/ceramint

La-, K- and Nb-doped $0.90(Bi_{0.5}Na_{0.5}TiO_3)$–$0.10PbTiO_3$

Sutin Kuharuangrong *

School of Ceramic Engineering, Suranaree University of Technology, Nakhon Ratchasima 30000, Thailand

Received 20 September 2005; received in revised form 4 May 2006; accepted 20 May 2006
Available online 12 September 2006

Abstract

Lanthanum, Potassium and Niobium have been selected as cation dopants to modify the relaxor characteristics of $0.90(Bi_{0.5}Na_{0.5}TiO_3)$–$0.10PbTiO_3$. The experimental results show that La lowers the phase transition temperatures and decreases the grain size. In contrast, the grain size of K-doped composition tends to increase. Furthermore, the maximum of dielectric permittivity and the Curie temperature increase as compared to those of La-doped material. La can improve the broadness of dielectric permittivity of $0.90(Bi_{0.5}Na_{0.5}TiO_3)$–$0.10PbTiO_3$. However, Nb is a better promising dopant for enhancing the relaxor behavior for this composition.

Keywords: C. Dielectric properties; Bismuth sodium titanate; Relaxor

1. Introduction

$Bi_{0.5}Na_{0.5}TiO_3$ (BNT) was first synthesized by Smolenskii and Agranovskaya [1] in 1959. A few years later, it was found to be ferroelectric from the polarization–electric field hysteresis loops [2]. In 1974, Sakata and Masuda [3] reported an antiferroelectric phase existed at 220 °C from dielectric measurement with an applied dc field. However, the optical and X-ray investigations [3,4] did not show any structural changes from the ferroelectric to the antiferroelectric phases. The maximum of dielectric permittivity [2,3,5,6] appeared around 325–335 °C and its value at a frequency of 10 kHz was 2600 [6]. The dielectric loss increased rapidly above this temperature.

Although most investigations have concentrated on the modifications of BNT for applications as piezoelectric and pyroelectric devices, this material is considered to be a good candidate for a high temperature relaxor. Doped with Pb [6], this material gives a higher dielectric permittivity and a lower transition temperature from ferroelectric to antiferroelectric phases as compared to unmodified BNT. However, this phase transition and the relaxor characteristics disappear as the amount of Pb increases to 17%. The reported morphotropic phase boundary of $Bi_{0.5}Na_{0.5}TiO_3$–$PbTiO_3$ (BNT–PT) is found between 15 and 17%Pb [6] since the structure changes from rhombohedral to tetragonal and relaxor characteristics disappear. Nevertheless, 10%Pb-doped BNT (BNT–10PT) is suitable composition to further modify for a stable high temperature dielectric. Most cation dopants have been selected to substitute in the A-site of this perovskite material. Sr and Ba dopants can increase the maximum dielectric permittivity of BNT–10PT but decrease its Curie temperature [3,7]. La lowers both phase transition temperatures of ferroelectric to antiferroelectric and antiferroelectric to paraelectric [8]. In addition, it decreases the dielectric permittivity of the composition. K has been investigated in a form of the solid solutions of $(1-x)Bi_{0.5}Na_{0.5}TiO_3$–$xBi_{0.5}K_{0.5}TiO_3$ system. The dielectric and piezoelectric properties including phase transition [9–11] of this system have been studied and the morphotropic phase boundary is reported at $x = 0.16$–0.20. In addition, a new intermediate compound exists at $0.20 \leq x \leq 0.40$. This is probably due to the larger size of K^+ than that of Na^+. Therefore, a partial solid solution of BNT–BKT can form within a limited amount of BKT. In this paper, the effects on the microstructure and dielectric properties of BNT–10PT from La, K and Nb dopants are presented. La and K are expected to substitute in the A-site and Nb in the B-site. The addition of K in this work is only small amount and far from the limited boundary for a formation of intermediate compound.

* Tel.: +66 44 224474; fax: +66 44 224462.
E-mail address: sutin@sut.ac.th.

0272-8842/$32.00
doi:10.1016/j.ceramint.2006.05.018

2. Experimental procedure

The following compositions were prepared in this work:

(a) 0.90($Bi_{0.5}Na_{0.5}TiO_3$)–0.10$PbTiO_3$ or BNT–10PT;
(b) 0.90($Bi_{0.45}La_{0.05}Na_{0.5}TiO_3$)–0.10$PbTiO_3$ or B45L5N5–10PT;
(c) 0.90($Bi_{0.48}La_{0.02}Na_{0.48}K_{0.02}TiO_3$)–0.10$PbTiO_3$ or B48L-2N48K2–10PT;
(d) 5%Nb-doped BNT–10PT;
(e) 10%Nb-doped BNT–10PT.

All specimens were prepared using ceramic powder processing technique and solid-state reaction. The powder was produced by ball-milling stoichiometric amounts of Bi_2O_3, TiO_2, PbO, Nb_2O_5, Na_2CO_3 and K_2CO_3, >99% purity from Aldrich. Lanthanum oxide (99.9% purity from Aldrich) was calcined at 1000 °C to decompose either hydroxide or carbonate, if existing, before weighing and mixing with other raw materials. The mixture was mixed by ball milling in a high density polyethylene bottle using zirconia balls and ethanol. After drying, the mixture was calcined in air and held at the reaction temperatures determined from the differential thermal analysis (DTA, Perkin-Elmer DTA7). The phases of calcined powder were analyzed by X-ray diffraction (XRD, Jeol JDX3530) using Cu Kα radiation before the disk specimens were formed by cold-isostatic press and put on the calcined powder in closed alumina crucibles before sintering at 1200 °C. Above this temperature, the shape distortion of some compositions started taking place attributing to liquid phase formation during sintering.

The microstructure of the sintered specimens was characterized by scanning electron microscope (SEM, Jeol JSM-5410LV). All cross-sectional areas of sintered compositions were polished and thermally etched before analysis.

The temperature dependence of the capacitance and dissipation factor of all compositions was measured by HP4192A Impedance Analyzer. The specimens were electroded with fired-on gold paste. All data were collected at different frequencies with an increasing temperature of 3 °C/min from room temperature to 400 °C.

3. Results and discussion

The differential thermal analysis of the milled raw materials for the compositions of BNT–10PT, B45L5N5–10PT, B48L2N48K2–10PT and 10%Nb-doped BNT–10PT is shown in Fig. 1. The results show that the exothermic peaks occur between 250 and 350 °C for all compositions, resulting from the decomposition. The data indicate that the reactions complete before 750 °C due to no additional peaks observed above this temperature. However, the higher calcination temperature and holding at the reaction temperatures are necessary to complete the reactions for a large amount of powder. In this work, calcining at 800 °C with a heating rate of 2 °C/min is used for all compositions. The calcined powder is identified by XRD and illustrated in Fig. 2. The results indicate that the pattern of B45L5N5–10PT has the same phase and structure as obtained from that of BNT–10PT. However, the patterns of B48L2N48K2–10PT and Nb-doped BNT–10PT show small peaks of 2θ around 30° and 56° indicating that the other phase exists in these compositions. This phase is possibly corresponding to pyrochlore or any intermediate phase, which always occurs in the Pb-perovskite compositions.

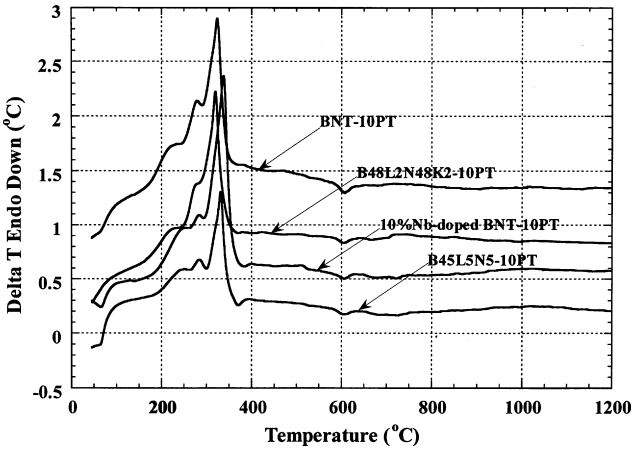

Fig. 1. DTA traces of mixed raw materials for the compositions of BNT–10PT, B45L5N5–10PT, B48L2N48K2–10PT and 10%Nb-doped BNT–10PT.

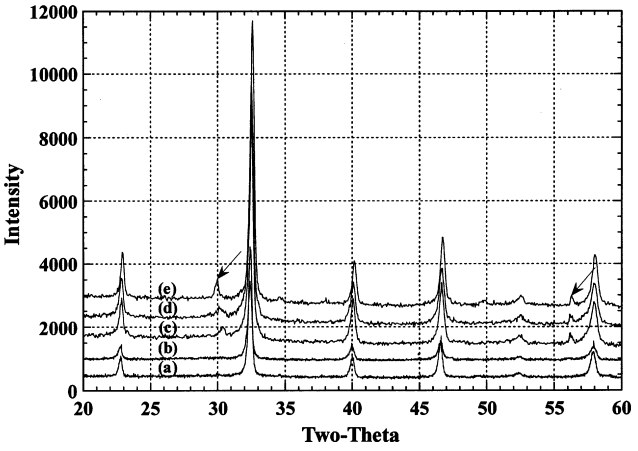

Fig. 2. XRD patterns at room temperature of: (a) BNT–10PT, (b) B45L5N5–10PT, (c) B48L2N48K2–10PT, (d) 5%Nb-doped BNT–10PT and (e) 10%Nb-doped BNT–10PT.

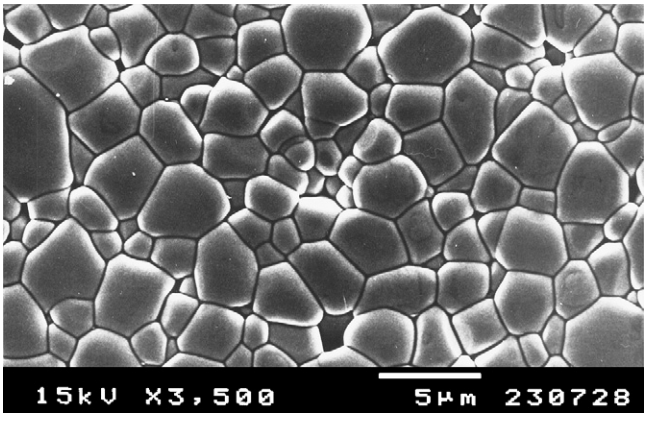

Fig. 3. SEM micrograph of sintered BNT–10PT.

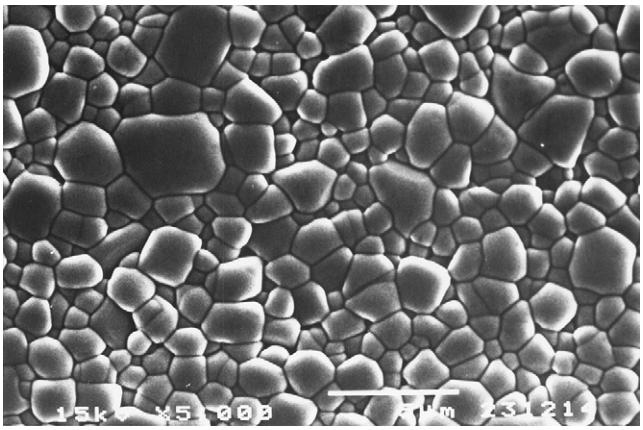

Fig. 4. SEM micrograph of sintered B45L5N5–10PT.

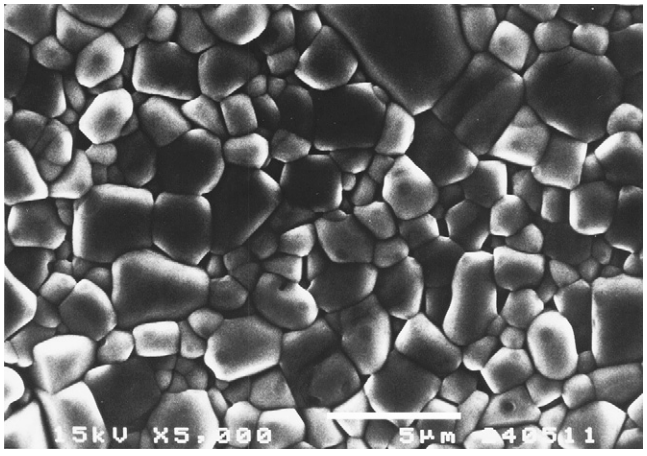

Fig. 5. SEM micrograph of sintered B48L2N48K2–10PT.

Figs. 3 and 4 represent SEM micrographs of the polished specimens of BNT–10PT and B45L5N5–10PT bulk materials. La can decrease the grain size of BNT–10PT as compared to K dopant (Fig. 5). It should be noted that the magnification used in Fig. 3 is different from that in Figs. 4 and 5. Figs. 6 and 7 show the photomicrographs of 5%Nb- and 10%Nb-doped BNT–10PT, respectively. The amount of Nb does not significantly affect the grain size. However, the grain size tends to reduce with an increasing amount of Nb.

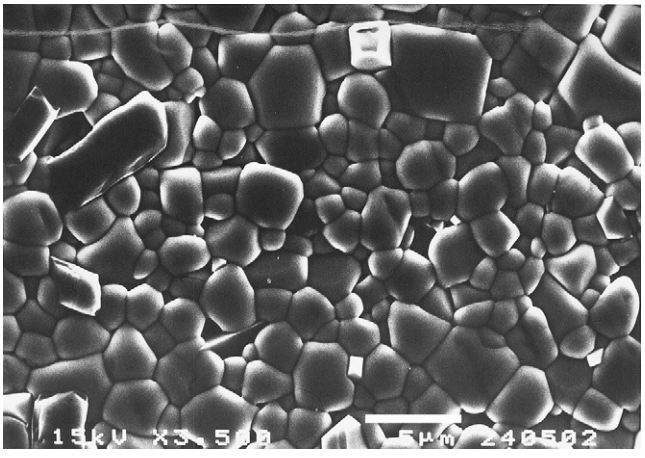

Fig. 6. SEM micrograph of sintered 5%Nb-doped BNT–10PT.

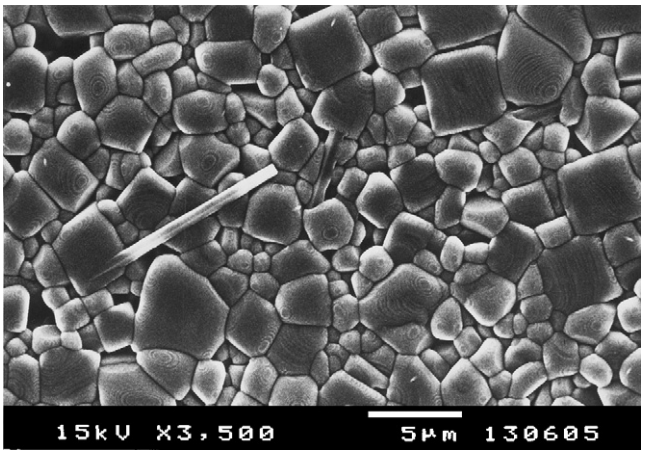

Fig. 7. SEM micrograph of sintered 10%Nb-doped BNT–10PT.

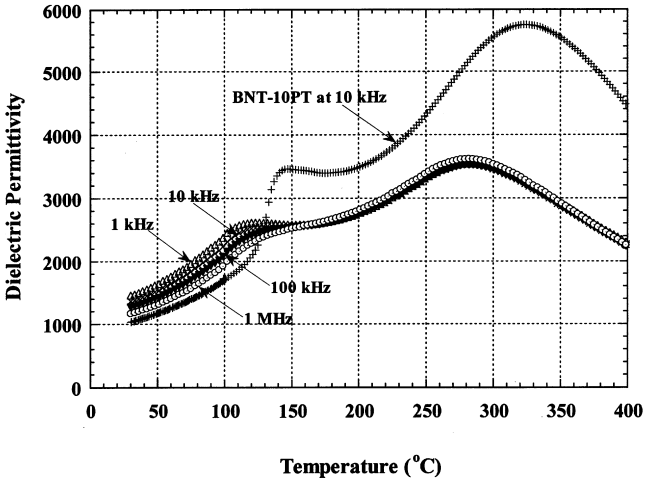

Fig. 8. Temperature and frequency dependence of the dielectric permittivity of B45L5N5–10PT and BNT–10PT at 10 kHz.

The results of the dielectric permittivity as a function of temperature and frequency of B45L5N5–10PT, B48L2N48K2–

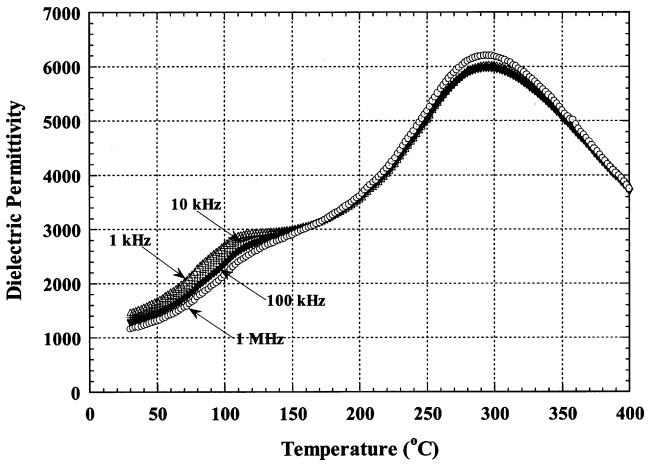

Fig. 9. Temperature and frequency dependence of the dielectric permittivity of B48L2N48K2–10PT.

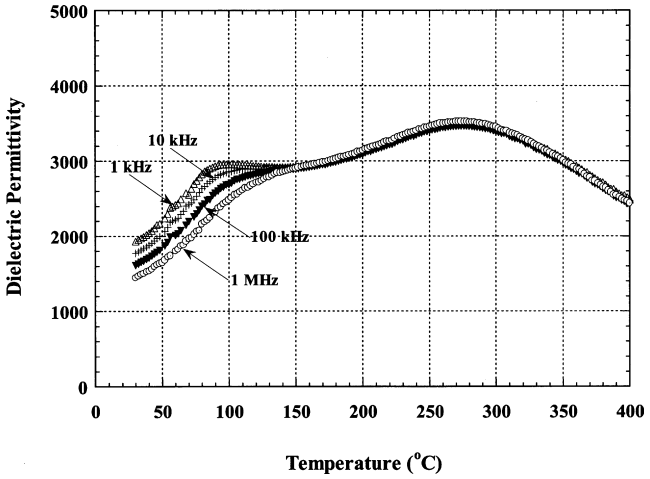

Fig. 10. Temperature and frequency dependence of the dielectric permittivity of 5%Nb-doped BNT–10PT.

10PT, 5%Nb- and 10%Nb-doped BNT–10PT are illustrated in Figs. 8–11, respectively. In addition, Fig. 12 shows the result of the dielectric permittivity of all compositions at a frequency of 10 kHz. All of them show a relaxor characteristic relaxation in which the dielectric permittivity at the first transition temperature displaces toward higher temperatures with increasing measuring frequency as shown in Figs. 8–11. Doped with La, both phase transition temperatures of BNT–10PT around 140 and 325 °C shift to lower temperatures at 115 and 282 °C, respectively. Furthermore, the result shows the decreasing dielectric permittivity of La-doped composition between these phase transition temperatures. In contrast to La, K can enhance the maximum of dielectric permittivity of BNT–10PT as displayed in Figs. 9 and 12. K also extends the antiferroelectric range to lower temperature. However, the broadness is reduced due to an increase of the difference between the dielectric permittivity of both phase transitions. With 5%Nb dopant, not only the first phase transition and the Curie temperatures of BNT–10PT shift toward lower temperatures but the maximum dielectric permittivity reduces from 5750 to 3480 as represented in Figs. 10 and 12. The broadness of BNT–10PT is obviously

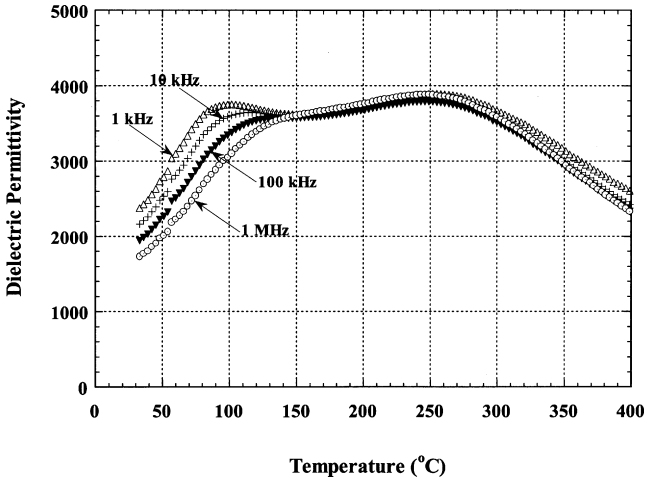

Fig. 11. Temperature and frequency dependence of the dielectric permittivity of 10%Nb-doped BNT–10PT.

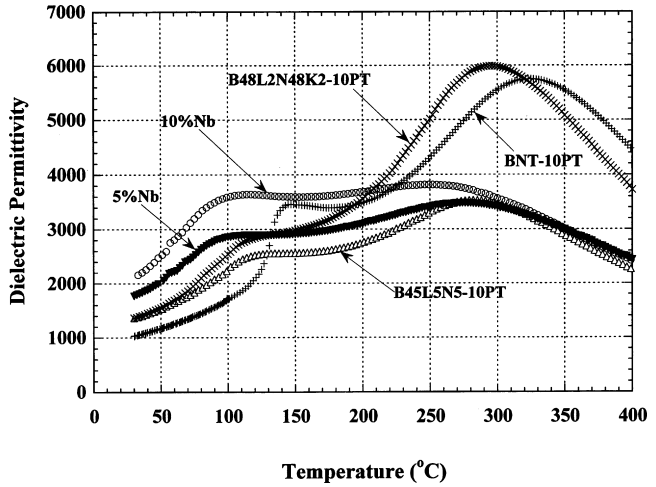

Fig. 12. Temperature dependence of the dielectric permittivity of BNT–10PT, B45L5N5–10PT, B48L2N48K2–10PT, 5%Nb- and 10%Nb-doped BNT–10PT at 10 kHz.

improved, suggesting that the effect of dopant type contributes to the broadening dielectric permittivity of BNT–10PT. With an increasing amount of Nb to 10% as shown in Figs. 11 and 12, the dielectric permittivity also increases and the difference of dielectric permittivity between the first transition temperature and the Curie point is reduced. This implies that the broadness can be improved as Nb content increases. The maximum of dielectric permittivity of 10%Nb-doped BNT–10PT at a frequency of 10 kHz is 3820 and the difference of dielectric permittivity between these two transition temperatures is 250. This indicates that a better relaxor characteristic of BNT–10PT can be obtained with an appropriate amount of Nb dopant.

The maximum of dielectric permittivity (K_{max}), the first transition temperature (T_1), the Curie point (T_c) and the difference of dielectric permittivity (ΔK) between these two temperatures for all compositions are summarized in Table 1. In addition, it includes the broadness parameter (δ) obtained from a plot of the dependence of $(1/K) - (1/K_{max})$ on $(T - T_c)^2$ [12,13]. The slope of this curve is determined to be the value of $(1/2K_{max}\delta^2)$. The results from Table 1 show the diffuseness of BNT–10PT with 5%Nb dopant has a higher value (136 °C) than that of BNT–10PT with 10%Nb (130 °C) and B45L5N5–10PT (120 °C). Fig. 13 shows plots of $(K_{max} - K)/K_{max}$ versus $(T - T_c)^2$ for those compositions, in which the dash lines represent the temperatures below T_c and the solid lines represent the temperatures above T_c of each composition. The gap between the dash and the solid lines exhibits the difference

Table 1
Maximum dielectric permittivity (K_{max}), the first transition temperature (T_1), the Curie point (T_c), the difference of dielectric permittivity (ΔK) between these two temperatures measured at 10 kHz and the broadness parameter (δ)

Composition	K_{max}	T_1 (°C)	T_c (°C)	$\Delta K_{(T_c - T_1)}$	δ (°C)
BNT–10PT	5750	140	325	$2345_{(185)}$	102
B45L5N5–10PT	3535	115	282	$1050_{(167)}$	120
B48L2N48K2–10PT	5990	112	294	$3200_{(182)}$	97
5%Nb-doped BNT–10PT	3480	94	274	$650_{(180)}$	136
10%Nb-doped BNT–10PT	3820	97	250	$250_{(153)}$	130

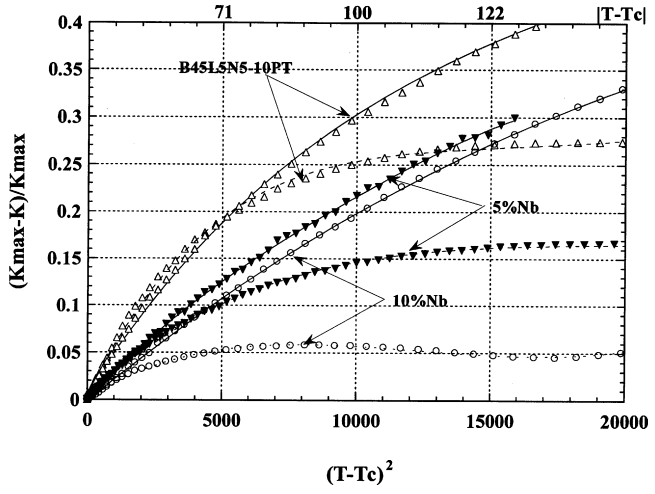

Fig. 13. Dependency of $(K_{max} - K)/K_{max}$ on $(T - T_c)^2$ of B45L5N5–10PT, 5%Nb- and 10%Nb-doped BNT–10PT at 10 kHz.

of dielectric permittivity between temperatures below and above T_c. The slope of each curve implies the difference of dielectric permittivity from its maximum dielectric. In other words, a steeper slope indicates less broadening dielectric permittivity. These results indicate BNT–10PT with 10%Nb dopant has more broadening dielectric permittivity than that with 5%Nb since the slope of dash line of 10%Nb doped BNT–10PT is lower than that of 5%Nb. Although the gap between the dash and the solid lines of 5%Nb is narrower than that of 10%Nb-doped BNT–10PT, the broadness of this base material is considered in the range of antiferroelectric phase between T_1 and T_c instead of paraelectric phase above T_c. This possibly affects the different broadness value from Table 1 which is determined above T_c.

The results of dissipation factor for all compositions at a frequency of 10 kHz are shown in Fig. 14. The loss tangent in a ferroelectric region depends on the dopant and its amount. K and Nb can raise the dissipation factor. Moreover, it increases with the amount of Nb. This effect is possibly related to the charge difference of Nb^{5+} from host Ti^{4+}, resulting in a formation of

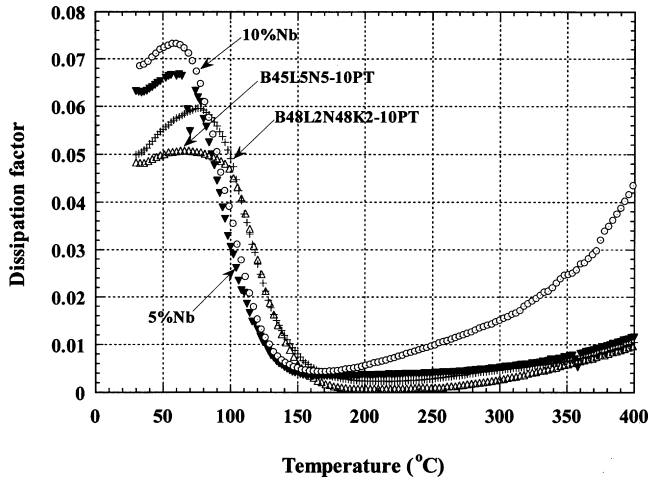

Fig. 14. Temperature dependence of the dissipation factor of B45L5N5–10PT, B48L2N48K2–10PT, 5%Nb- and 10%Nb-doped BNT–10PT at 10 kHz.

defect to conserve the electrical neutrality. This defect can also raise the dielectric loss of this composition. Obviously, as illustrated in Fig. 14, at higher temperature the dissipation factor of 10%Nb-doped composition increases rapidly due to the high temperature conduction from the point defect as usually occurs above T_c in the dielectric materials [14].

4. Conclusions

La inhibits grain growth of BNT–10PT and shifts the antiferroelectric region to lower temperature. In contrast, the grain size of K-doped composition tends to increase and the maximum dielectric permittivity is raised. With Nb dopant, the relaxor characteristic of BNT–10PT can be improved as compared to those of La and K dopants. An increase in Nb content increases the broadness of BNT–10PT but insignificantly affects the grain size.

Acknowledgement

This work was supported from Thailand Research Fund.

References

[1] G.A. Smolenskii, A.I. Agranovskaya, Dielectric polarization of a number of complex compounds, Sov. Phys. Solid State 1 (1959) 1429–1437.
[2] G.A. Smolenskii, V.A. Isupov, A.I. Agranovskaya, N.N. Krainik, New ferroelectrics of complex composition IV, Sov. Phys. Solid State 2 (1961) 2651–2654.
[3] K. Sakata, Y. Masuda, Ferroelectric and antiferroelectric properties of $(Na_{0.5}Bi_{0.5})TiO_3$–$SrTiO_3$ solid solution ceramics, Ferroelectrics 7 (1974) 347–349.
[4] V.A. Isupov, I.P. Pronin, T.V. Kruzina, Temperature dependence of birefringence and opalescence of the sodium bismuth titanate crystals, Ferroelectr. Lett. 2 (1984) 205–208.
[5] I.P. Pronin, P.P. Syrnikov, V.A. Isupov, V.M. Egorov, N.V. Zaitseva, Peculiarities of phase transitions in sodium–bismuth titanate, Ferroelectrics 25 (1980) 395–397.
[6] S. Kuharuangrong, W.A. Schulze, Characterization of $Bi_{0.5}Na_{0.5}TiO_3$–$PbTiO_3$ dielectric materials, J. Am. Ceram. Soc. 79 (1996) 1273–1280.
[7] S. Kuharuangrong, W.A. Schulze, Compositional modifications of 10%-Pb-doped $Bi_{0.5}Na_{0.5}TiO_3$ for high-temperature dielectrics, J. Am. Ceram. Soc. 78 (1995) 2274–2278.
[8] S. Kuharuangrong, Effect of La and K on the microstructure and dielectric properties of $Bi_{0.5}Na_{0.5}TiO_3$–$PbTiO_3$, J. Mater. Sci. 36 (2001) 1727–1733.
[9] I.P. Pronin, N.N. Parfenova, N.V. Zaitseva, V.A. Isupov, G.A. Smolenskii, Phase transitions in solid solutions of sodium–bismuth and potassium–bismuth titanates, Sov. Phys. Solid State 24 (1982) 1060–1062.
[10] A. Sasaki, T. Chiba, Y. Mamiya, E. Otsuki, Dielectric and piezoelectric properties of $(Bi_{1/2}Na_{1/2})TiO_3$–$(Bi_{1/2}K_{1/2})TiO_3$ systems, Jpn. J. Appl. Phys. 38 (1999) 5564–5567.
[11] H. Nagata, M. Yoshida, Y. Makiuchi, T. Takenaka, Large piezoelectric constant and high Curie temperature of lead-free piezoelectric ceramic ternary system based on bismuth sodium titanate–bismuth potassium titanate–barium titanate near the morphotropic phase boundary, Jpn. J. Appl. Phys. 42 (2003) 7401–7403.
[12] T.R. Shrout, U. Kumar, M. Megheri, N. Yang, S.J. Jang, Grain size dependence of dielectric and electrostriction of PMN-based ceramics, Ferroelectrics 76 (1987) 479–487.
[13] V.A. Isupov, Ferroelectrics having a weakly broadened phase transition, Sov. Phys. Solid State 28 (1986) 1253–1254.
[14] R.E. Newnham, Structure–property relations in ceramic capacitors, J. Mater. Educ. 5 (1983) 947–982.